

# Using an onion like neutron scattering instrument model to quickly optimize design parameters

Thomas Huegle

Neutron Technologies Division, Spallation Neutron Source, Oak Ridge National Laboratory, Oak Ridge, TN 37831, USA

Email: [hueglet@ornl.gov](mailto:hueglet@ornl.gov)

---

This manuscript has been authored by UT-Battelle, LLC, under contract DE-AC05-00OR22725 with the US Department of Energy (DOE). The US government retains and the publisher, by accepting the article for publication, acknowledges that the US government retains a nonexclusive, paid-up, irrevocable, worldwide license to publish or reproduce the published form of this manuscript, or allow others to do so, for US government purposes. DOE will provide public access to these results of federally sponsored research in accordance with the DOE Public Access Plan (<http://energy.gov/downloads/doe-public-access-plan>).

---

## Abstract

When designing a neutron scattering instrument, one of the major challenges is the many parameters, generally interdependent, within the optimization. In this paper we describe an approach using McStas<sup>1-3</sup> to quickly get a good overview of how changes in instrument parameters will impact neutron scattering instrument performance.

*Keywords: McStas; Mantid; neutron scattering; neutron scattering instruments; neutron optics; python*

## 1. Introduction

When designing a neutron scattering instrument, many decisions about the instrument parameters will need to be made for both the primary flight path (e.g. flight path length, maximum divergence of a guide system) and the instrument itself (layout of detectors, pixel size of detector, etc.). McStas offers a way to simulate instrument performance as a function of these parameters, but attempting to fill in the multidimensional matrix of parameters by individual simulations is time-consuming work (e.g. “how does the resolution at 1 Å d-spacing of an 8 mm wide detector pixel at 45° scattering angle, 1.5m from the sample position change when we increase the flight path distance from 35m to 40m while keeping the divergence of the guide constant”).

Using the McStas component “Monitor\_nD” to occupy the space surrounding the sample position with detector shells, and McStas’ ability to provide its output as a Mantid-compatible NeXus event file<sup>4-7</sup> allows us to analyze the spectrum of each individual pixel and extract any metric one might be interested in from time-of-flight (TOF) data. This (in combination with e.g. python’s matplotlib) results in condensed graphical representations of the various parameters’ effects. In this article, we focus on instrument

resolution as the metric to consider, but any other metric extractable from a neutron scattering spectrum could be used.

## 2. Parameters to consider

### 2.1. Resolution

The most common representation of the resolution function of a TOF neutron scattering instrument used for diffraction is

$$\frac{\Delta Q}{Q} = \sqrt{\left(\frac{\Delta t}{t}\right)^2 + \left(\frac{\Delta L}{L}\right)^2 + (\Delta\theta \cot \theta)^2} \quad [1]$$

It is derived from the fact that an instrument's resolution is dependent on its uncertainty in Time of Flight ( $t$ ), flight path length ( $L$ ), and scattering angle ( $\theta$ ). The nominal flight path length from the moderator surface should be fairly well known, but its uncertainty will be increased by factors like the sample size, the physical extent of the moderator, or the fact that the moderator surface is often viewed at an angle. The ambiguity in time of flight is caused by the fact that neutrons of otherwise identical properties will be emitted from the moderator surface with a time distribution during a pulse. The scattering angle is influenced by both the angle of the incoming neutron (divergence) and the fact that any detector pixel will have a physical size (solid angle). The fact that the resolution function contains the cotangent of  $\theta$ , which goes rapidly towards infinity as the scattering angle  $\theta$  approaches 0, means that any instrument will be severely limited in its resolution in the forward scattering direction.

### 2.2. Primary flight path

One main factor contributing to instrument resolution originating from the primary flight path is the length of the flight path, influencing the  $\Delta L/L$  term in Equation [1]. The other major factor concerns the divergence of the neutron beam, usually described by the extent of the angular distribution of neutrons reaching the sample. In its simplest form without an optical system such as a neutron guide, this corresponds to the angle from the sample position to the edges of the moderator, something often referenced as "natural divergence". If a guide system is introduced, this becomes somewhat more complex: the *maximum* divergence (corresponding to the maximal angle at which a neutron can reach the sample) is described by the angle between sample and guide exit. However, since neutron guide efficiency is heavily wavelength dependent (which in turn is modified by guide shapes), the actual divergence is a wavelength dependent distribution, in which case the full width at half maximum (FWHM) of this distribution can be used to describe divergence. Guide optimization is one of the most important steps of instrument design, but also one of the most complex<sup>8,9</sup>, since any change in a guide's divergence distribution might necessitate change in the detector layout.

### 2.3. Detector layout

Significant effort in the planning of a neutron scattering instrument will be allocated to the detector layout: How much detector coverage is required (and how can that be optimized with respect to detector cost)? Should the detectors be arranged in a circle around the sample or in one flat panel at a certain angle? And what would the optimal distance be? At which pixel size will we fully utilize the best resolution of the instrument in its current configuration? And what happens to all these parameters once anything is changed about the primary flight path? A comparably simple way to answer these questions through McStas simulations is to fill the maximum solid angle extent of an instrument with successive detectors, use the `restore_neutron` option in each of them (which means a neutron will continue its path after being detected), and see how changes affect the range of all detector layouts at once. The `Monitor_nD` component offers a convenient way of doing this by using the “banana” option, which sets a pixelated detector in a cylindrical shape around a position. Furthermore, the `Monitor_nD` component allows McStas to export its results as a NeXus event file, which means the user can analyze the spectrum of each individual pixel for any metric of interest (e.g. FWHM of a certain diffraction peak) in an easily scriptable way.

### 3. Example

To illustrate the process, we chose the design considerations for the VERDI instrument, a diffractometer optimized for magnetic structure studies of both powder and single crystals which is in its conceptual design stage for the planned second target station at Oak Ridge National Laboratory.<sup>10</sup> The first parameters that need to be roughly determined before further optimization are flight path length, maximal divergence of a guide concept, detector type, and detector layout. A test case instrument using input files available in the current McStas release can be found in the appendix of this publication.

#### 3.1. Source

The `SNS_source` component can simulate a full moderator pulse. This is especially important for resolution calculations because it includes the emission time distribution that determines the  $\Delta t/t$  term of the resolution function (Eq. [1]).

#### 3.2. Detector and instrument setup

As mentioned before, this approach uses the `Monitor_nD` component of McStas. We will for now focus on the in-plane detectors: Each shell of the detector is only 1cm high and consists of 1 pixel in height. Two typical shells are defined:

```
COMPONENT nD_Mantid_1 = Monitor_nD(  
  yheight = 0.01, radius = 1.0,  
  options="mantid, banana, theta limits=[5,170] bins=360, y bins=1,  
  neutron pixel min=0 t, list all neutrons",  
  restore_neutron=1)  
AT (0,0,0) RELATIVE sampleMantid
```

```

1 COMPONENT nD_Mantid_2 = Monitor_nD(
2   yheight = 0.01, radius = 1.25,
3   options="mantid, banana, theta limits=[5,170] bins=450, y bins=1,
4   neutron pixel min=360 t, list all neutrons",
5   restore_neutron=1)
6   AT (0,0,0) RELATIVE sampleMantid
7

```

Notable parameters of the detectors are:

- nD\_Mantid\_#: the naming scheme of the detectors if they are to be used to record Mantid readable event data is hard wired.
- Yheight: As previously stated, we focus on the in-plane scattering in this example.
- Radius: The radius is increased by 25cm each shell
- Options:
  - Mantid: enable Mantid compatible event data mode
  - Banana: detector is circular around position
  - Theta limits = [5,170]: detector coverage ranges from 5° to 170°. Do not allow detector to overlap primary beam, otherwise an inordinate quantity of irrelevant neutron events will be saved.
  - Theta bins = 360: number of bins in theta. Varies with detector radius for a fixed pixel width.
  - Y bins = 1: only one pixel high (Note: McStas 2.4 does not handle the export of pixels to Nexus format correctly, which prevents this option under normal circumstances. The issue has been resolved in McStas 2.5)
  - Neutron pixel min: starting pixel id. Has to be adjusted accumulatively, otherwise data from different detector will be attributed to the same pixel id.

A detector array of multiple concentric shells can now be used in an instrument file. In this example a simple setup consisting of the appropriate source (component `SNS_source`) and a sample will suffice. Since the metric of interest is the resolution of a powder diffractometer, the `Powder1` component which creates a single scattering vector (e.g. d-spacing = 2 Å) is chosen.

### 3.3. Simulation

The McStas simulation is run using the necessary commands to enable Mantid readable NeXus output<sup>6</sup>. The precision of follow-on analysis is dependent on sufficient statistics being recorded in each individual pixel. Therefore, rather good statistics are necessary. A rule of thumb is that the output file should be at least 1GB in size. The exact number of neutron histories to achieve this depends on factors like source focusing and the actual number of detector pixels in the instrument.

### 3.4. Analysis

1 Analysis of the data is performed using the Mantid suite. In-depth documentation on the specifics of each  
2 algorithm is available in the Mantid documentation<sup>5</sup>. The analysis can be done either manually in  
3 Mantidplot or scripted in Python using the Mantid library. An example for an analysis script can be found  
4 in the appendix of this publication.

#### 6 *Converting TOF data*

7 Prior to histogramming the event data must be converted to appropriate units. “ConvertUnits” allows  
8 us to do so, and “Rebin” produces histogrammed data. The result of this is now one spectrum per  
9 detector pixel (identified by pixel ID).

#### 11 *Extracting a metric*

12 “FindPeaks” is an algorithm that analyses spectra, has various fitting functions, and produces a  
13 spreadsheet containing (amongst others) pixel IDs and peak widths (FWHM). If a more custom analysis is  
14 desired to extract a specific metric, one can also easily loop over the histogrammed data using Python:  
15 “readX(i)”, “readY(i)” and “readE(i)” extract data from Mantid workspaces as numpy arrays,  
16 where “i” represents the pixel ID.

#### 18 *Obtaining the pixel coordinates*

19 “PreprocessDetectorsToMD” creates a spreadsheet that contains (amongst other useful  
20 information) the detector geometry: pixel IDs and corresponding coordinates.

#### 22 *Visualizing the data*

23 Using the two spreadsheets that assign peak width and coordinates to a given pixel ID, respectively, it is  
24 now straightforward to plot the resulting data using any program of choice, e.g. python’s matplotlib. The  
25 resolution is calculated as  $\Delta d/d$  (peak width/peak position) and is used as the color scale (Figure 1, left).  
26 As mentioned above (‘Extracting a metric’), it is also possible to access the spectra of individual pixels  
27 (Figure 1, right).

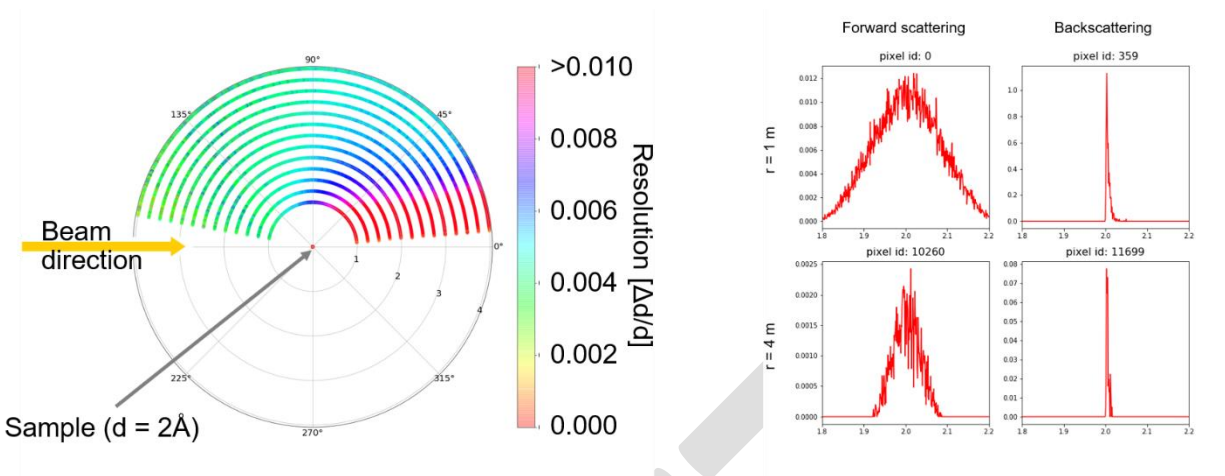


Figure 1: Resolution of a  $2\text{\AA}$  peak as a function of angle and distance to the sample position. Primary flight path: 40m, Divergence:  $0.2^\circ$ . Left side: Top down view. Detector radius: 1m - 4m (25cm increments). Detector coverage:  $5^\circ$  -  $170^\circ$  (8mm pixel width). Right side: spectrum of four distinct pixels. Pixel 0: inner ring, forward scattering. Pixel 359: inner ring, backscattering. Pixel 10260: outer ring, forward scattering. Pixel 11699: outer ring, backscattering.

This gives a good overview of the resolution space around a sample for a given flight path configuration and can help making an informed decision about the starting point for a possible detector layout.

### 3.5. Changing the primary flight path

With the resolution space of the secondary flight path analyzable like this, one can now make changes to the primary flight path and observe how that influences the secondary flight path. The length of the flight path is changed easily in the McStas instrument files. A way to estimate the influence of divergence on the instrument resolution is to calculate the maximum divergence that a guide could deliver (e. g. the angle between guide exit width and sample) and extrapolate from there to the extent of a neutron source that would deliver the same divergence (Figure 2). This is of course a rough approximation that neglects any wavelength dependent guide effects but will give a good starting point for detailed guide calculations.

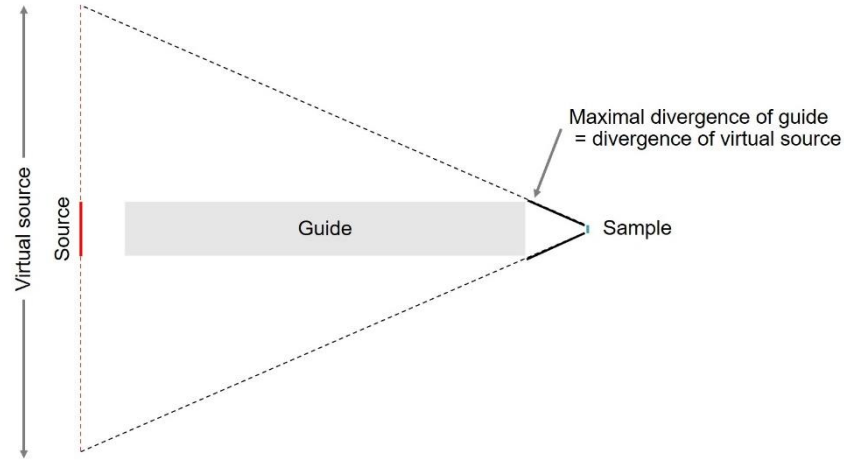


Figure 2: Approximating beam divergence of a guide by modeling a virtual source.

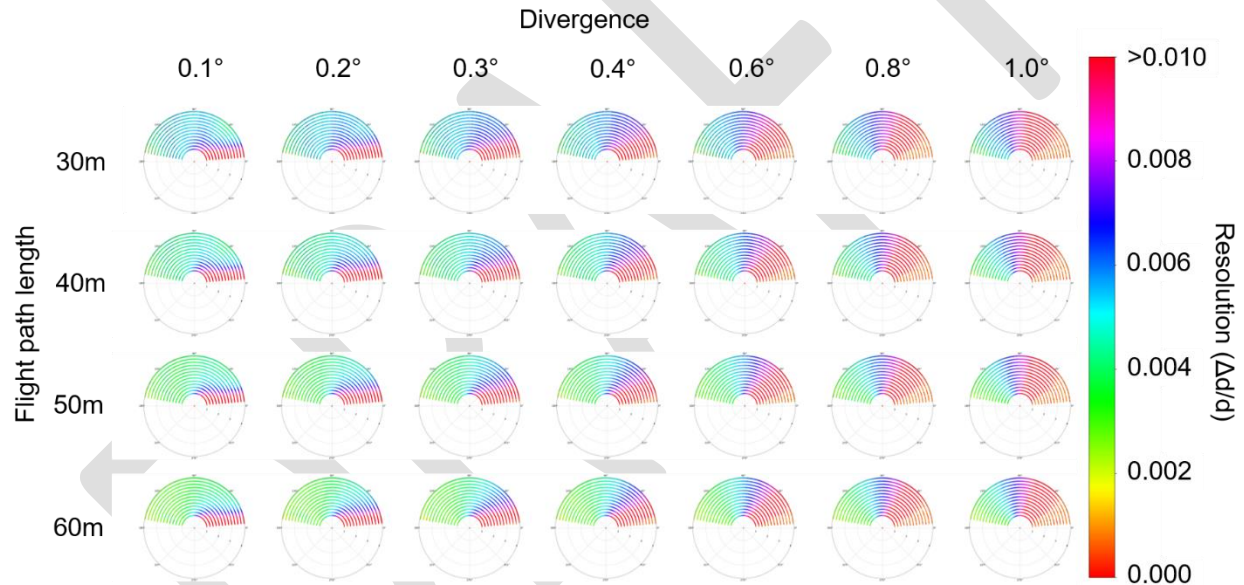


Figure 3: Effects of variation in primary flight path length and divergence on instrument resolution. Details of each individual graph are identical to Figure 1. At high divergences ( $\sim 0.6^\circ$ ) the peak in forward scattering direction becomes too wide for the algorithm to recognize it. This leads to a) cases where data points are missing and b) cases where noise is mistaken for a (much sharper) peak. In the graphic representation, this leads to a) a drop in color intensity and b) a perceived shift to impossibly good resolutions ( $\Delta d/d < 0.001$ ). The resolution in this area can safely be assumed to be worse than 0.01. Using much wider wavelength spectrum bin sizes can remedy this problem at the expense of detail in the high-resolution areas of the data. See also Figure 1, right side.

The resulting graph (Figure 3) shows two distinct trends: the flight path length increases the “best possible” resolution in backscattering, whereas the divergence influences the “worst possible” resolution in forward scattering. This is very much in accord with “common knowledge”. Since the instrument in question will focus partly on the investigation of low Q phenomena, it will be limited by the “worst” resolution in forward scattering much more than the “best” resolution in backscattering. The starting

point for the simulations that will follow now was therefore chosen to be 40 m primary flight path, a guide of approximately  $0.2^\circ$  divergence (in high resolution mode), and (upon a more detailed look at Figure 1) a detector layout that could be a circle of  $\sim 2.5$  m diameter or possibly a logarithmic spiral that extends from  $\sim 1.5$  m in backscattering to  $\sim 3.5$  m in forward scattering (Figure 4).

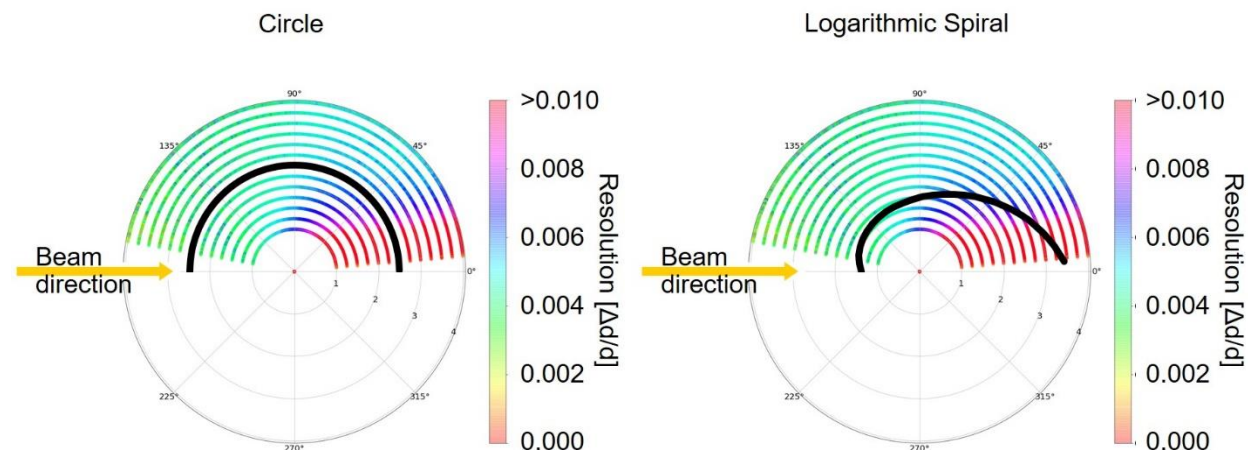


Figure 4: Possible detector layouts (thick black line) for an instrument of 40 m flight path length and  $0.2^\circ$  divergence. Left: Circular layout (radius = 2.5 m). Right: Logarithmic spiral layout (backscattering distance  $\approx 1.2$  m, forward scattering distance  $\approx 3.5$  m).

#### 4. Conclusion

A concentric shells ‘onion’ type instrument is a convenient and highly illustrative way of exploring the interdependence of primary and secondary flight path. This provides a good, quick method to independently confirm focusing and resolution effect ideas as a cross check for analytical instrument development concepts. Using McStas to create event data enables post processing in Mantid as an independent step. While the examples presented in this publication focus on resolution as the guiding metric, other metrics can be chosen (e.g. intensity of a specific signal). Simulating 3-dimensional instruments consisting of shells is theoretically possible but will be limited in practice by the file size necessary to have decent statistics per pixel spectrum. For metrics that are not as pixel size dependent as resolution, this might be mitigated by increasing pixel size.

#### Acknowledgements

This material is based upon work supported by the U.S. Department of Energy, Office of Science, Office of Basic Energy Sciences under contract number DE-AC05-00OR22725.

This research used resources at the Spallation Neutron Source, a DOE Office of Science User Facility operated by the Oak Ridge National Laboratory.



This research used resources of the Compute and Data Environment for Science (CADES) at the Oak Ridge National Laboratory, which is supported by the Office of Science of the U.S. Department of Energy under Contract No. DE-AC05-00OR22725.

## References

1. Willendrup, P., Farhi, E. & Lefmann, K. McStas 1.7 - a new version of the flexible Monte Carlo neutron scattering package. *Phys. B Condens. Matter* **350**, E735–E737 (2004).
2. P, W., E, F., E, K., U, F. & K, L. McStas: Past, present and future. *J. Neutron Res.* 35–43 (2014). doi:10.3233/JNR-130004
3. Lefmann, K. & Nielsen, K. McStas, a general software package for neutron ray-tracing simulations. *Neutron News* **10**, 20–23 (1999).
4. Arnold, O. *et al.* Mantid—Data analysis and visualization package for neutron scattering and  $\mu$  SR experiments. *Nucl. Instrum. Methods Phys. Res. Sect. Accel. Spectrometers Detect. Assoc. Equip.* **764**, 156–166 (2014).
5. *Mantid (2013): Manipulation and Analysis Toolkit for Instrument Data.; Mantid Project.*
6. Nielsen, T. R., Markvardsen, A. J. & Willendrup, P. McStas and Mantid integration. *J. Neutron Res.* **18**, 79–92 (2016).
7. Klosowski, P., Koennecke, M., Tischler, J. . & Osborn, R. NeXus: A common format for the exchange of neutron and synchrotron data. *Phys. B Condens. Matter* **241–243**, 151–153 (1997).
8. Bentley, P. M., Kennedy, S. J., Andersen, K. H., Martin Rodríguez, D. & Mildner, D. F. R. Correction of optical aberrations in elliptic neutron guides. *Nucl. Instrum. Methods Phys. Res. Sect. Accel. Spectrometers Detect. Assoc. Equip.* **693**, 268–275 (2012).
9. Bentley, P. M. & Andersen, K. H. Optimization of focusing neutronic devices using artificial intelligence techniques. *J. Appl. Crystallogr.* **42**, 217–224 (2009).
10. Galambos, J. D. *et al. Technical Design Report, Second Target Station.* (2015). doi:10.2172/1185891